ACS APPLIED MATERIALS & INTERFACES

Forum Article

www.acsami.org

Voltage Gain in Lithiated Enolate-Based Organic Cathode Materials by Isomeric Effect

Sébastien Gottis,[†,‡,⊥] Anne-Lise Barrès,[§,⊥] Franck Dolhem,*[,‡,⊥] and Philippe Poizot*[,§,⊥]

[†]Laboratoire de Réactivité et Chimie des Solides (LRCS), UMR CNRS 7314, Université de Picardie Jules Verne, 33 rue Saint-Leu, 80039 Amiens Cedex, France

[‡]Laboratoire de Glycochimie, des Antimicrobiens et des Agroressources (LG2A), FRE CNRS 3517, Université de Picardie Jules Verne, 33 rue Saint-Leu, 80039 Amiens Cedex, France

[§]Institut des Matériaux Jean Rouxel (IMN), UMR CNRS 6502, 2 rue de la Houssinière, B.P. 32229, 44322 Nantes Cedex 3, France

[⊥]Réseau sur le Stockage Electrochimique de l'Energie (RS2E), FR CNRS 3459, 80039 Amiens Cedex, France

Supporting Information

ABSTRACT: Li-ion batteries (LIBs) appear nowadays as flagship technology able to power an increasing range of applications starting from small portable electronic devices to advanced electric vehicles. Over the past two decades, the discoveries of new metal-based host structures, together with substantial technical developments, have considerably improved their electrochemical performance, particularly in terms of energy density. To further promote electrochemical storage systems while limiting the demand on metal-based raw materials, a possible parallel research to inorganic-based batteries consists in developing efficient and low-polluting organic electrode materials. For a long time, this class of redox-active materials has been disregarded mainly due to stability issues but, in recent years, progress has been made demonstrating that organics undeniably exhibit considerable assets. On the basis of our ongoing research aiming at elaborating lithiated organic cathode materials, we report herein on a chemical approach that takes advantage of the positive potential shift when switching from para to ortho-position in the dihydroxyterephthaloyl system. In practice, dilithium (2,3-dilithium-oxy)-terephthalate compound ($Li_4C_8H_2O_6$) was first produced through an eco-friendly synthesis scheme based on CO_2 sequestration, then characterized, and finally tested electrochemically as lithiated cathode material vs. Li. This new organic salt shows promising electrochemical performance, notably fast kinetics, good cycling stability and above all an average operating potential of 2.85 V vs. Li^+/Li^0 (i.e., +300 mV in comparison with its para-regioisomer), verifying the relevance of the followed strategy.

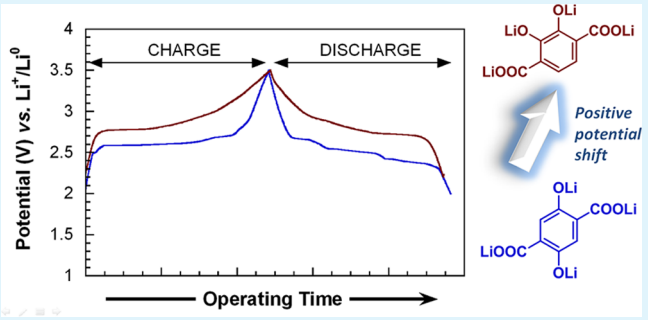

KEYWORDS: *organic cathode materials, dihydroxybenzene dilithium moiety, isomeric effect, organic battery*

INTRODUCTION

The necessity to integrate renewable electricity both on and off the grid, coupled with eagerness of the electric automotive industry and electronic manufacturers, have markedly increased the need for high-performance and affordable electrochemical generators, particularly the rechargeable ones. Therefore, the world production of secondary batteries is expected to keep on growing for a long time. As an example, the current market of lithium-ion batteries represents alone a production of billions of units per year.[1] A possible brake for the future could be related to the chemistries used until now. Indeed, most traditional batteries are based on the redox chemistry of inorganic species (mainly metals),[2] of which some are scarce natural resources, often costly (even toxic) and energy greedy at the process level.

In this context, we had already underlined that redox-active organic compounds could play an important role in the forthcoming battery technologies[3] including also what we now call "post Li-ion". Different arguments can be put forward in favor of organic batteries. First, organic molecules are composed of quite naturally abundant chemical elements (C, H, N, O, S, in particular) and if properly designed, they could be generated from renewable resources (biomass). Second, organics can operate from dissolved to solid state (including polymers) in aqueous or nonaqueous electrolytes making them versatile in terms of electrochemical storage devices. Third, the richness of organic chemistry provides great opportunities for finding novel and innovative electrode materials with specific properties including the elaboration of multimodal systems (e.g., dual electrochemical/chemical rechargeability[4]). Quite importantly, this multiplicity of chemical combinations at the

Special Issue: New Materials and Approaches for Electrochemical Storage

Received: November 30, 2013
Accepted: February 17, 2014
Published: March 4, 2014

dx.doi.org/10.1021/am405470p | ACS Appl. Mater. Interfaces 2014, 6, 10870−10876

Scheme 1. General Key Redox-Active Organic Systems and Their Related Charge Transfer Steps (adapted from Hünig's classification[6])[a]

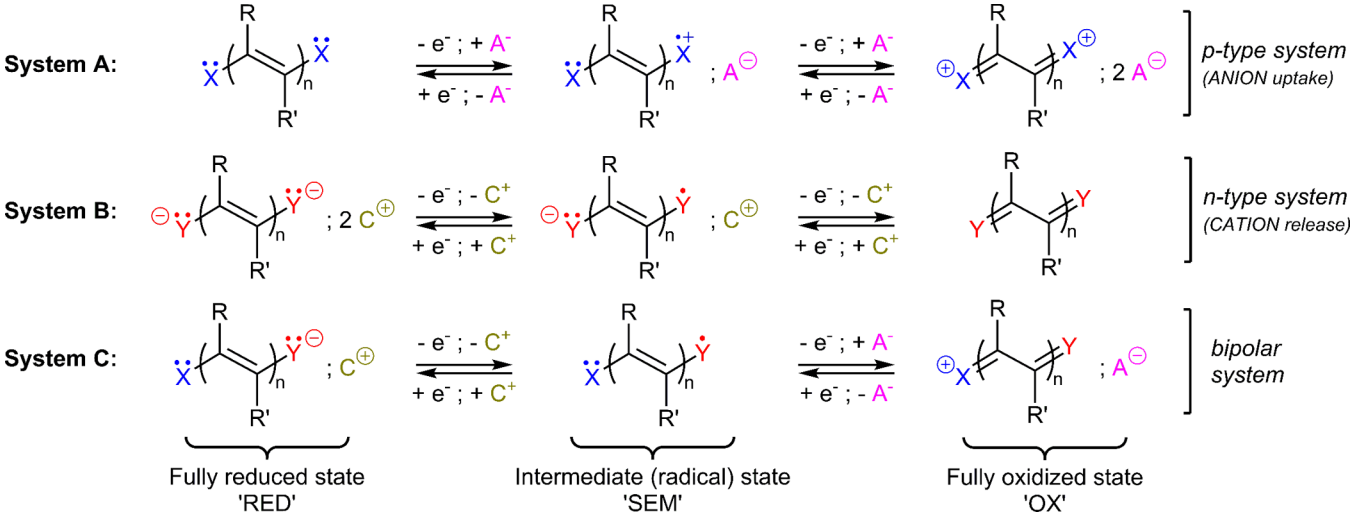

[a]X/Y could be N, O, S, P, π-systems but also carboxylate, anhydride, or amide functional groups as demonstrated these last few years in the field of rechargeable batteries (see for instance refs 7−14); R, R′ being potentiality integrated within the same cyclic structure. Note that the Syst. B appears as the most relevant for developing organic Li-ion batteries being balanced with cations (C^+).

molecular level also gives rise to an incomparable tool for (i) tuning the redox potential of conjugated systems[5] and (ii) promoting reversible multielectron reactions as rationalized by Hünig long time ago.[6] On this latter point, Scheme 1 recalls the three general key organic structures that lead to multistage organic redox systems in solution (deriving from Hünig's classification), which appeared also to us as quite relevant to design efficient organic electrode materials for electrochemical energy storage applications.

In short, it seems now established that there is a room for this class of redox-active compounds; see the excellent reviews recently published on the topic[15,16] and the great achievements realized specifically with organic radical batteries (ORBs).[17−21] Nevertheless, much remains to be done especially to achieve simultaneously high energy/power density and high cyclability in a fully integrated organic Li-ion cell.

A significant part of our research in this field over the last few years, however, was focused instead on Wurster-type redox structures, which integrate the general Syst. (Scheme 1) using oxygen as the end group (Y = O).[3,4,22−26] Although such a system leads to effective electrochemical potentialities, a first shortcoming lies in the difficulty to find efficient lithiated enolate structures ('RED' form of the Syst. B) able of being reversibly delithiated (charged) at a sufficiently high potential.[15,16,27] However, we have recently demonstrated that dilithium (2,5-dilithium-oxy)-terephthalate (denoted Li_4-*p*-DHT)[4] constitutes a robust lithiated cathode material able to exhibit quite good electrochemical behavior including fast kinetics and good cyclability. Searching to increase the operating potential value of this promising organic structure (and therefore its specific energy density), a simple strategy would be to take advantage of the positive potential shift when switching from para to ortho-position in the quinone/hydroquinone moiety, a well-known phenomenon in molecular electrochemistry.[28,29] For example, a positive potential shift of 240 mV is noted in acetonitrile medium between the two semiquinone/hydroquinone redox couples (Table 1). In this article, we specifically report on the elaboration and the electrochemical assessment of dilithium (2,3-dilithium-oxy)-terephthalate (denoted Li_4-*o*-DHT), which is simply the ortho-regioisomer of Li_4-*p*-DHT, where extended conjugation is also expected at different oxidation states.

Table 1. Half-wave Potential ($E_{1/2}$) of Both 1,2- and 1,4-Benzoquinone Measured vs. SCE in 0.1 M NEt_4ClO_4/Acetonitrile at 25°C.[29]

	$E_{1/2}$ ($Q/Q^{\bullet-}$)	$E_{1/2}$ ($Q^{\bullet-}/Q^{2-}$)
1,2-benzoquinone	−0.31	−0.90
1,4-benzoquinone	−0.51	−1.14

EXPERIMENTAL MATERIALS AND METHODS

General Methods. ^1H and ^{13}C NMR spectra were recorded on a Bruker AVANCE III at 400 and 100.7 MHz respectively; chemical shifts (δ) are given in ppm relative to TMS. DMSO-d_6 was purchased from Eurisotop Company (purity higher than 99.5%). Infrared spectra were performed with a FTIR Bruker Vertex 70. Pellets were prepared by thoroughly mixing the organic compound with spectroscopic-grade potassium bromide at 1% (w/w). ESI-HRMS experiments were performed in the negative ion mode on a Q-TOF Ultima Global instrument (Waters-Micromass, Manchester, UK) equipped with a pneumatically assisted electrospray ion source (Z-spray) and an additional sprayer for the reference compound (LockSpray). The TG-DSC measurements were carried out with a Netzsch STA 449 F3 Jupiter coupled with mass spectrometry for gas analysis. TG/DSC analyses were systematically obtained using a heating rate of 5 °C min^{-1}. Temperature-controlled X-ray powder diffraction (TRXRPD) experiments were performed on a Bruker D8 Advance diffractometer equipped with an Anton Parr Chamber HTK 1200 N high-temperature attachment. Data were collected in Bragg−Brentano geometry with a Cu-anode X-ray source operated at 40 kV and 40 mA. The Cu K_β radiation was filtered by means of a Ni foil. The experiment was carried out under nitrogen flow with a step of 0.016724° and an acquisition time of 1.2 s per step (heating rate of 0.2 °C s^{-1}).

Synthesis Procedures. 1,2-Dihydroxybenzene (catechol or benzene-1,2-diol) was supplied by Carlo Erba (≥99%), lithium hydroxide ($LiOH·H_2O$) by Fluka (≥99%), potassium hydrogen carbonate (99%) by Sigma-Aldrich and lithium carbonate by Riedel-

dx.doi.org/10.1021/am405470p | ACS Appl. Mater. Interfaces 2014, 6, 10870−10876

de Haën (≥99%). Concentrated hydrochloric acid (36 wt %) was purchased from Fisher Scientific.

2,3-Dihydroxyterephthalic Acid (H_4-o-DHT). 1,2-Dihydroxybenzene (3.386 g, 31 mmol) and potassium hydrogen carbonate, previously dried under vacuum at 60 °C overnight (9.237 g, 93 mmol, 3 equiv), were ground with a mortar and pestle then placed in a Parr reactor system (300 mL), which was degassed under vacuum prior to be filled with CO_2 until the inner pressure at room temperature reached 20 bar. The Parr reactor was then heated overnight to 200 °C leading to a final autogenerated pressure reaching 45 bar. The crude material was dissolved in water (10 mL) and acidified with HCl (to pH 2) to precipitate 2,3-dihydroxyterephthalic acid. After filtration, the recovered solid was suspended in 100 mL of water, then LiOH (aq., sat.) was added dropwise until complete solubilization. The solution was acidified once more and filtered off. The creamy precipitate was dried under vacuum at 50 °C for one day resulting in pure 2,3-dihydroxyterephthalic acid monohydrated (5.199 g, 78%). ^{1}H NMR (400 MHz, DMSO-d_6) δ (ppm) 7.28 (s, 2H, H arom.). ^{13}C NMR (100 MHz, DMSO-d_6) δ (ppm): 171.52 (*C*OOH), 150.79 (*C*–OH), 118.55 (*C*–COOH), 116.75 (*C*H). IR (KBr pellet): ν_{max}/cm^{-1} 3523–2525 (ν O–H, ν C–H), 1949, 1659 (ν C═O), 1622, 1569, 1486–1396 (ν C═C), 1346, 1323, 1227–1170 (ν C–O, ν OC–OH, δ O–H), 889–753 (ν C–H), 660, 559, 493, 432 cm^{-1} (see spectra in the Supporting Information). MS (ESI) (*m*/*z*): [M-H]$^-$ calcd for $C_8H_5O_6$, 197.0086; found, 197.0078.

Dilithium 2,3-Dihydroxyterephthalate (Li_2-o-DHT·3.7 H_2O). Water (20 mL) was added to a mixture of 2,3-dihydroxyterephthalic acid monohydrate (1 g, 4.62 mmol) and lithium carbonate (0.342 g, 4.62 mmol) previously ground with a mortar and pestle. The mixture was stirred until complete dissolution. The as-obtained solution was then poured into a watch glass and water was removed by slow evaporation in air, overnight. A gray powder was recovered corresponding to Li_2-o-DHT·3.7 H_2O (1.264 g, 99% yield). ^{1}H NMR (400 MHz, DMSO-d_6) δ (ppm) 6.92 (s, 2H, H arom.), 3.36 (s, H_2O). ^{13}C NMR (100 MHz, DMSO-d_6) δ (ppm) 171.88 (COOLi), 153.17 (*C*–OH), 120.49 (*C*–COOLi), 115.77 (*C*H). IR (KBr pellet): ν_{max}/cm^{-1} 3503–3200 (ν O–H), 2820–2455 (ν C–H), 1648 (ν C═O), 1600, 1572, 1483–1413 (ν C═C), 1351 (ν OC–OLi), 1275 (ν C–OH), 1220 (δ O–H), 1151, 896, 834–655 (ν C–H), 524, 483, 441 cm^{-1} (see spectra in the Supporting Information). MS (ESI) (*m*/*z*): [M^{2-}, Li$^+$]$^-$ calcd, 203.0168; found: 203.0171.

Dilithium (2,3-Dilithium-oxy)-terephthalate (Li_4-o-DHT). In a glovebox, hydrated dilithium 2,3-dihydroxyterephthalate (300 mg, 1.43 mmol) was ground with a mortar and pestle then placed in a drying glass oven (Buchi B-585 glass-oven Kugelrohr) and heated during 16 h at a real temperature of 245 °C (250 °C on the display). This retro-Kolbe–Schmitt reaction produced a greenish-yellow powder of pure Li_4-o-DHT (120.1 mg, quantitative yield) and vapors of catechol, which condensed as uncolored crystals in the cool part of the oven. The formation of Li_4-o-DHT was confirmed by NMR after a derivatization reaction based on a full reprotonation step: 4 drops of H_2SO_4 (concentrated) were added to a heterogeneous solution of Li_4-o-DHT (25 mg) in DMSO-d_6 (1 mL) resulting in a homogeneous brown-colored solution. Both ^{1}H and ^{13}C NMR spectra correspond to pure 2,3-dihydroxyterephthalic acid. ^{1}H NMR (400 MHz, DMSO-d_6+H_2SO_4) δ (ppm): 11.91 (s, H acid), 7.13 (s, 2H, H arom.). ^{13}C NMR (100 MHz, DMSO-d_6+H_2SO_4) δ (ppm): 173.05 (COOH), 152.19 (*C*–OH), 120.37 (*C*–COOH), 118.30 (*C*H). IR (KBr pellet): ν_{max}/cm^{-1} 1566 (ν C═O), 1501–1442 (ν C═C), 1386 (ν OC–OLi), 1242 (ν C–OLi), 1149, 1014, 952, 862–738 (ν C–H), 679, 597, 496 cm^{-1} (see spectra in the Supporting Information).

Electrochemical Study. Electrochemical measurements were performed in conventional Swagelok-type cells using a Li metal disc as negative electrode and a fiberglass separator soaked with 1 M $LiPF_6$ solution (in ethylene carbonate:dimethyl carbonate/1:1 in volume ratio) as the electrolyte. As previously described for Li_4-*p*-DHT,[4] the positive composite electrode was prepared without binder in an argon-filled glovebox by grounding with a mortar and pestle powder of Li_4-o-DHT along with 50% of carbon black in mass (typically, Ketjenblack EC-600JD from AkzoNobel); the carbon content of the final electrode being 33% in mass. All cells were cycled in galvanostatic mode using a MPG-2 system (Bio-Logic S.A., Claix, France) at a typical rate of one lithium ion exchanged in 5 h (denoted 1 Li$^+$/5 h).

RESULTS AND DISCUSSION

From a synthesis point of view, we realized that our synthesis process previously developed for Li_4-*p*-DHT production[4] was also suitable, after appropriate adjustments, for the preparation of the ortho-regioisomer, with the 1,2-dihydroxybenzene (catechol) structure being the key reagent in this case instead of 1,4-dihydroxybenzene (Figure 1). Although catechol is

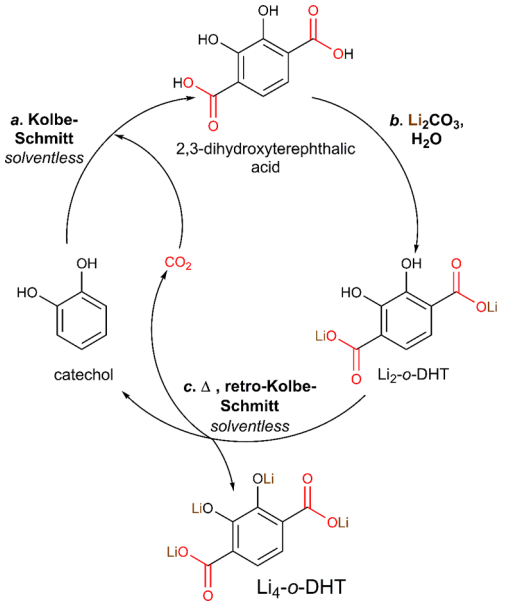

Figure 1. Synthesis process used for Li_4-o-DHT. The closed-loop process based on a retro-Kolbe-Schmitt step was originally developed for the synthesis of the para-isomer (Li_4-*p*-DHT).[4] During the thermal rearrangement, 1,2-dihydroxybenzene (catechol) is vaporized then condensed making a reintroduction in step a possible.

naturally and widely available in wildlife and flora,[30−33] the corresponding contents are too small for substantial extraction. Accordingly, its industrial production is rather based on the hydroxylation of phenol thanks to hydrogen peroxide. Nevertheless, another synthetic route does exist by starting with D-glucose using first *Escherichia coli* bacteria in water followed by a simple thermolysis.[34] Basically, no strong alkali nor expensive metals are needed during the whole process. The 2,3-dihydroxyterephthalic acid was readily obtained from the catechol (step a) by using a variant of the Kolbe-Schmitt and Marasse reaction.[35] In our experiment, we used a Parr reactor system filled with a mixture of hand ground catechol and potassium hydrogen carbonate, which was degassed under vacuum before it was filled with pure carbon dioxide. The potassium hydrogen carbonate plays two distinctive roles in this reaction. First, as a base, it initiates the formation of catecholate derivatives and the complexation of CO_2 for the selective ortho-substitution. Second, the thermal decomposition properties of potassium hydrogen carbonate over 100–120 °C help to increase the partial pressure of CO_2 in the reactor as the reaction proceeds.

This solventless methodology trapped 2 mols of carbon dioxide per catechol and offered exclusively the 2,3-dihydroxyterephtalic acid (H_4-o-DHT) as monohydrated phase with a

very good yield of 78% (see Figure S1 in the Supporting Information). Afterward, dilithium 2,3-dihydroxyterephthalate (Li_2-*o*-DHT) was simply recovered by neutralization with Li_2CO_3 (see Figure S2 in the Supporting Information). However, thermal analysis coupled with mass spectrometry evidenced the hydrated state of the as-prepared Li_2-*o*-DHT with a weight loss of 24.1% till ~130 °C corresponding to 3.7 water molecules per mole (Figure 2).

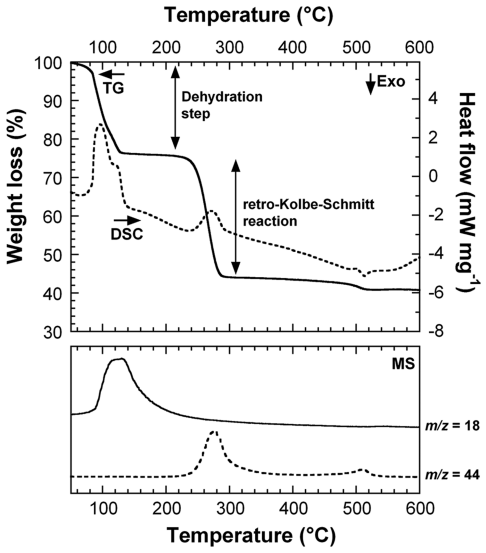

Figure 2. Thermogravimetric (TG) and differential scanning calorimetry (DSC) traces of dilithium 2,3-dihydroxyterephthalate obtained under argon at a heating rate of 5 °C min^{-1} combined with mass spectrometry (MS) measurements (m/z 18 is ascribed to H_2O and 44 to CO_2).

Beyond the dehydration process, a second abrupt step is observed on the TG curve associated with CO_2 release, which is consistent with the expected thermal intermolecular rearrangement for producing Li_4-*o*-DHT and catechol (50/50 in molar ratio) as summarized in Scheme 2.

The occurrence of the retro-Kolbe–Schmitt process was further confirmed by X-ray thermodiffractometry. The series of patterns collected from room temperature (RT) to 300 °C is shown in Figure 3. The crystalline Li_2-*o*-DHT·3.7 H_2O first underwent a phase transition during dehydration process (from RT to 200 °C) leading to an intermediate phase corresponding to the anhydrous compound. As expected, this phase transition occurred at similar temperature range as the dehydration process evidenced by thermal analysis (Figure 2). Another phase transition occurs above 200 °C leading to the formation of a thermally stable phase from 245 to 300 °C in agreement with the formation of Li_4-*o*-DHT through the retro-Kolbe Schmitt process. Note that an isotherm performed at 245 °C for 6 h clearly demonstrates the thermal stability of the as-

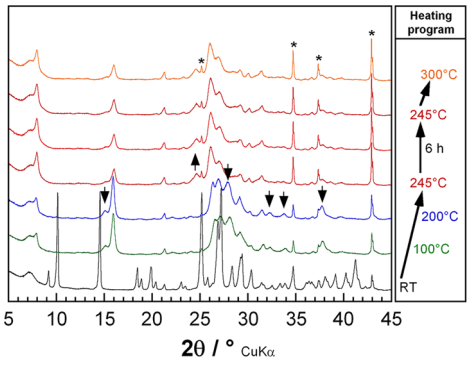

Figure 3. TRXRPD experiment performed under nitrogen flow at a heating rate of 0.2 °C s^{-1}. Arrows correspond to emergence (upside) or disappearance (downside) of Bragg peaks from anhydrous Li_2-*o*-DHT to the formation of the Li_4-*o*-DHT phase (* corresponds to peaks emanating from the sample holder). Note that an isotherm step at 245 °C during 6 h was included in the heating program.

obtained phase. In comparison with previous X-ray data regarding the formation of Li_4-*p*-DHT from the same reaction pathway,[4] evolutions of patterns between anhydrous and Li_4-*o*-DHT phases appear less obvious. Nevertheless, emergence of new Bragg peaks and disappearance of others (assigned with arrows in the Figure 3) together with the evolution of intensities, incontestably differentiate the anhydrous Li_2-*o*-DHT from the emergence of Li_4-*o*-DHT. To synthesize this phase at the lab scale, a typical batch of ~0.3 g of Li_2-*o*-DHT·3.7 H_2O was heated at a real temperature of 245 °C in a drying glass oven (Kugelrohr) under inert atmosphere. After a 15 h period of annealing, the sample lost ~60% in weight, whereas its pristine grayish color turned to greenish-yellow. As expected, small crystals of pure catechol were recovered in the cool part of the oven and then recycled. Finally, the obtainment of Li_4-*o*-DHT was finally confirmed by NMR after a derivatization reaction (see Figure S3 in the Supporting Information).[4] It is worth noting that this second successful synthesis confirms the potential of this solvent-less method centered on the thermal concerted retro-Kolbe–Schmitt rearrangement, which could be applied for producing other analogues or even other counterions such as Na or K, for instance.

For the sake of comparison, the electrochemical investigation of Li_4-*o*-DHT compound was performed vs. Li in Swagelok-type cells according to a similar procedure to the one previously reported for Li_4-*p*-DHT testing.[4] After a preliminary screening, typical electrochemical measurements consisting of galvanostatic cycling tests within the 3.2–2.2 V potential window were performed at a typical cycling rate of one Li^+ exchanged in 5 h. As for the para-regioisomer, it is worth noting that Li_4-*o*-DHT is also able to reversibly intercalate Li^+ at low potential thanks to the redox-activity of carboxylate groups. Figure 4a shows the typical potential–composition (E–x) trace restricted to the first five cycles. As expected, this regioisomer exhibits also an

Scheme 2. Thermal Concerted Retro-Kolbe–Schmitt Rearrangement of Li_2-*o*-DHT (anhydrous) for Producing Li_4-*o*-DHT; Catechol/Carbon Dioxide Secondary Products Being Released in Gas Phase

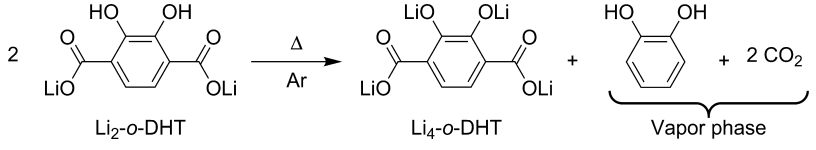

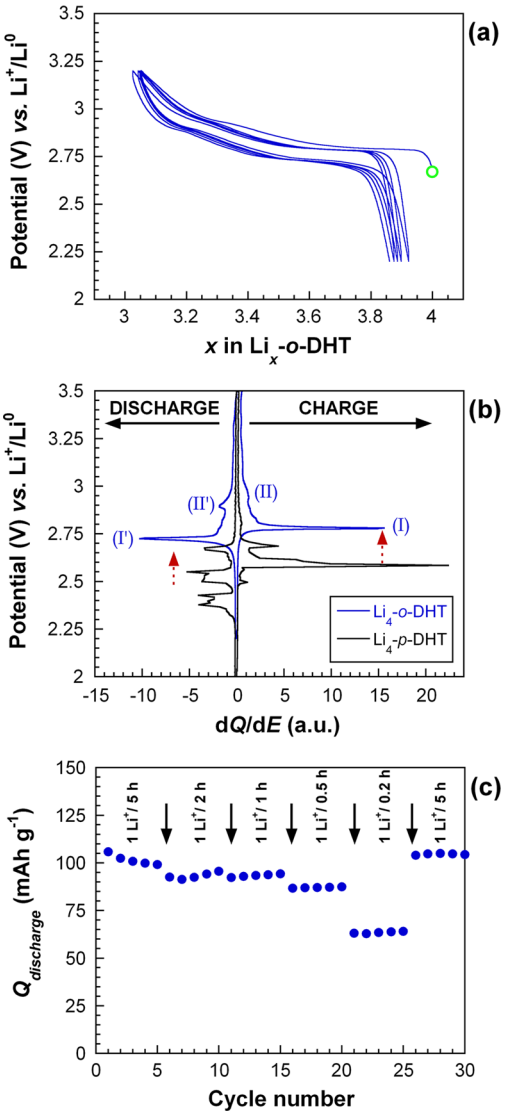

Figure 4. (a) First five cycles of a Li half-cell using Li_4-*o*-DHT as the positive electrode material (carbon additive: 33% in mass of the final electrode) and galvanostatically cycled at 1 Li^+/5 h. The green circle indicates the starting potential, $E_{I=0}$ = 2.65 V vs. Li^+/Li^0. (b) Superimposition of the potential vs. differential capacity curve (second cycle) for both Li_4-*o*-DHT and Li_4-*p*-DHT regioisomers. Red arrows point out the positive potential shift. (c) Corresponding specific capacity in discharge vs. cycle number for current rate changes ranging from 1 Li^+/5 h to 1 Li^+/0.2 h.

efficient reversible charging−discharging profile. During the first delithiation process, the oxidation curve shows a succession of two plateaus located at 2.80 and 2.95 V, respectively, together with solid-solution domains involving an apparent one-electron overall process (Δx = 0.98 for the first charge, Q = 117 mAh g^{-1}) as previously observed with Li_4-*p*-DHT.[4] These electrochemical features can be more accurately visualized on a potential vs. differential capacity curve where two principle reversible peaks are observed, denoted (I/I′) and (II/II′), respectively (Figure 4b). This series of electrochemical steps is almost symmetrically recovered during the subsequent reduction process with a very weak polarization effect (around 50 mV) even lower than for Li_4-*p*-DHT. Note that such a low value is quite rare for an organic material working as positive lithiated electrode. However, the real value-added of this regioisomer in respect to Li_4-*p*-DHT is the gain in terms of average operating potential, which has now reached 2.85 V vs. Li^+/Li^0 (2.55 V for Li_4-*p*-DHT, ΔE ~300 mV). Again, a better visualization of this positive potential shift can be readily obtained by a simple comparison of the respective potential vs. differential capacity curves of the two regioisomers (Figure 4b). Accordingly, this new experimental result confirms well our initial expectations and validates the fact that the positive potential shift well-known in solution when switching from para to ortho-position in the quinone/hydroquinone moiety[5,28,29] is qualitatively maintained in the solid state. To further probe the capability of this electrochemical process different cycling rates ranging from 1 Li^+/5 h to 1 Li^+/0.2 h were applied (Figure 4c). The capacity is slowly decreasing as the rate is increasing till 1 Li^+/0.5 h. By applying a current equivalent to 1 Li^+/0.2 h, the capacity fade is higher but the capacity value is still maintained at 63 mAh g^{-1}. Then, when the current is getting back to a cycling rate of 1 Li^+/5 h, the initial capacity retention is recovered at an average value of 105 mAh g^{-1}. At this point, although the design of the composite electrode architecture was not optimized because the active material used in the present study was neither carbon-coated nor mixed with a binder, this regioisomer exhibits promising electrochemical properties.

However, as with Li_4-*p*-DHT, it is worth noting that this ortho-regioisomer exhibits also an apparent electrochemical reactivity restricted to $\Delta x \approx 1$ although the two-electron reaction is basically expected for producing the corresponding quinonic form (i.e., Syst. B with Y = O, 'OX' form) as shown in Scheme 3.

Shortly after the publication of our article dedicated on the electrochemical properties of Li_4-*p*-DHT and its O_2-rechargeability properties,[4] Chen's group reported another study focused on this particular materials (also denoted Li_4DHTPA) but prepared according to a different synthesis approach.[36] Their results pointed out that only a strong decrease in particle size (i.e., use of nanosheets) enables to reach approximately the expected full capacity ($Q_{exp.}$ > 220 mAh g^{-1}; 241 mAh g^{-1} expected). However, the typical potential-composition profiles reported in this article are featureless (no obvious plateau) in contrast with our measurements, which could also indicate a different crystal structure compared to our material. Attempts to decrease the particle size of the as-prepared Li_4-*o*-DHT are currently in progress.

Finally, having previously demonstrated that a solid-state autoxidation reaction spontaneously occurred with Li_4-*p*-DHT in the presence of oxygen,[4] we decided to test this ortho-regioisomer as well since it still operates at an average potential below 3 V vs. Li^+/Li^0. Experimentally, the chemical stability in air was first assessed by FTIR spectroscopy thanks to a series of spectra recorded at different exposure times (Figure 5a). As for the para-regioisomer, a clear transition occurs involving the appearance of new peaks (dotted lines) as a color change proceeds. Another relevant experiment to further confirm the occurrence of this autoxidation phenomenon was to monitor the mass uptake under O_2 as function of time. The approach consisted in repeating and adapting our previous thermal analysis measurement (Figure 2). In short, a new sample of Li_2-*o*-DHT·3.7 H_2O was heated in the TG/DSC apparatus at a rate of 5 °C min^{-1} under argon until 350 °C to produce in situ Li_4-*o*-DHT. After cooling, the neutral gas stream was replaced by pure oxygen (Figure 5b). The monitoring of the mass evolution with time shows unambiguously a continuous increase that reaches almost 10% in 48 h (~5% in 4 h). By considering an

Scheme 3. Expected Delithiation/Lithiation Process Based on Two-Electron Reaction in Li_4-*o*-DHT and Li_4-*p*-DHT, Respectively

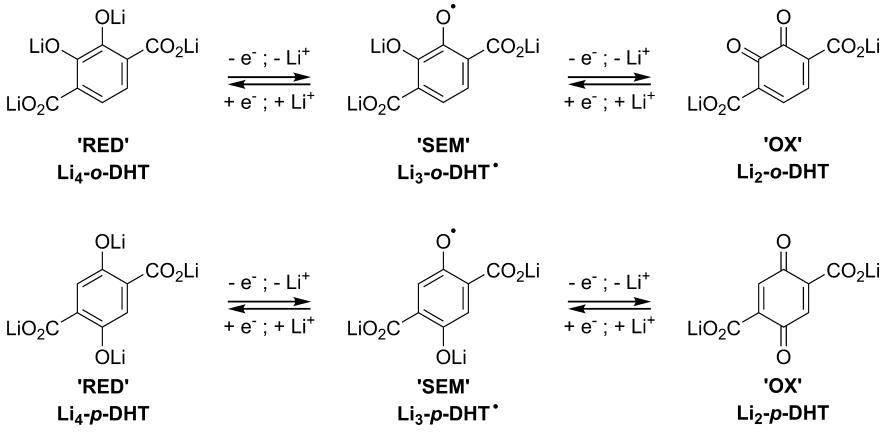

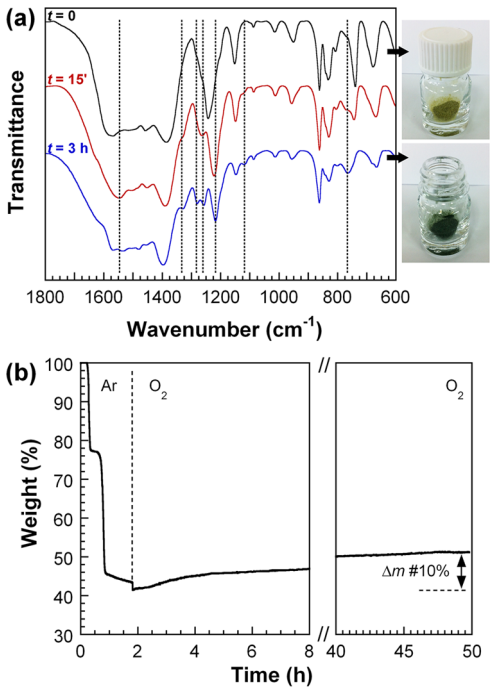

Figure 5. (a) Evolution of both FTIR spectra and color appearance of the pristine Li_4-*o*-DHT powder after exposition in ambient atmosphere. The pristine greenish-yellow color turned to greenish-blue. (b) Specific TG analysis for probing the mass gain of Li_4-*o*-DHT under oxygen flow. The initial period under Ar corresponds to the in situ production of Li_4-*o*-DHT from Li_2-*o*-DHT·3.7 H_2O as shown in Figure 2. Then, the neutral gas stream was replaced by pure oxygen.

oxidation process that leads to the semiquinone radical formation, a mass uptake of 14% is expected. In light of these results, this study was also the occasion to demonstrate that this ortho-regioisomer can therefore be perceived as another organic electrode material able to promote the oxygen reduction reaction (ORR).

CONCLUSION

A novel redox-active lithiated dihydroxyterephthaloyl derivative was synthesized through an original process that includes the chemical sequestration of carbon dioxide. As already successfully used in the case of Li_4-*p*-DHT synthesis, this new example demonstrates that the retro-Kolbe–Schmitt reaction reprents an efficient route for preparing alkali salts of *β*-hydroxy acid (BHA). For instance, sodium analogues can be readily obtained through the same method. More specifically, this study was the occasion to verify the occurrence of the positive potential shift at the solid state when switching from para to ortho-position in the dihydroxyterephthaloyl system. Comparison of typical chronopotentiograms of both Li_4-*o*-DHT and Li_4-*p*-DHT isomers showed a potential variation of nearly 300 mV. Additionally, interesting electrochemical performance was observed with fast kinetics and good capacity retention upon cycling. At this time, a limitation to one-electron process per ring is observed, which calls for further investigations to reach the theoretical capacity (241 mAh g^{-1}). Lastly, the ability of Li_4-*o*-DHT to act as a scavenger of molecular oxygen was also demonstrated in agreement with thermodynamics because its redox-activity is still centered below 3 V vs. Li^+/Li^0.

ASSOCIATED CONTENT

Supporting Information

Additional data: ^1H NMR, ^{13}C NMR, and IR spectra of H_4-*o*-DHT, Li_2-o-DHT·3.7 H_2O, and Li_4-*o*-DHT. This material is available free of charge via the Internet at http://pubs.acs.org.

AUTHOR INFORMATION

Corresponding Authors

*E-mail: franck.dolhem@u-picardie.fr. Tel.: +33 3 22 82 79 39. Fax: +33 3 22 82 75 60.

*E-mail: philippe.poizot@cnrs-imn.fr. Tel.: +33 2 40 37 39 41. Fax: +33 2 40 37 39 95.

Notes

The authors declare no competing financial interest.

ACKNOWLEDGMENTS

This work was partially funded by the Région Pays de la Loire. The authors deeply thank Steven Renault (currently at Uppsala University, Sweden) for fruitful discussions and his valuable comments as well as Stéphane Grolleau (IMN) and Grégory Gachot (LRCS) for complementary experiments.

REFERENCES

(1) Scrosati, B.; Garche, J. Lithium Batteries: Status, Prospects and Future. *J. Power Sources* **2010**, *195*, 2419–2430.

(2) *Handbook of Battery Materials*, 2nd ed.; Daniel, C., Besenhard, J. O., Eds.; Wiley-VCH: Weinheim, Germany, 2011.

(3) Poizot, P.; Dolhem, F. Clean Energy New Deal for a Sustainable World: From non-CO_2 Generating Energy Sources to Greener Electrochemical Storage Devices. *Energy Environ. Sci.* **2011**, *4*, 2003−2019.
(4) Renault, S.; Gottis, S.; Courty, M.; Chauvet, O.; Dolhem, F.; Poizot, P. A Green Li−organic Battery Working as a Fuel Cell in Case of Emergency. *Energy Environ. Sci.* **2013**, *6*, 2124−2133.
(5) Zhu, X.-Q.; Wang, C.-H. Accurate Estimation of the One-Electron Reduction Potentials of Various Substituted Quinones in DMSO and CH_3CN. *J. Org. Chem.* **2010**, *75*, 5037−5047.
(6) Deuchert, K.; Hünig, S. Multistage Organic Redox Systems-A General Structural Principle. *Angew. Chem., Int. Ed.* **1978**, *17*, 875−886.
(7) Armand, M.; Grugeon, S.; Vezin, H.; Laruelle, S.; Ribière, P.; Poizot, P.; Tarascon, J.-M. Conjugated Dicarboxylate Anodes for Li-ion Batteries. *Nat. Mater.* **2009**, *8*, 120−125.
(8) Abouimrane, A.; Weng, W.; Eltayeb, H.; Cui, Y.; Niklas, J.; Poluektov, O.; Amine, K. Sodium Insertion in Carboxylate Based Materials and their Application in 3.6 V Full Sodium Cells. *Energy Environ. Sci.* **2012**, *5*, 9632−9638.
(9) Renault, S.; Mihali, V. A.; Brandell, D. Optimizing the Electrochemical Performance of Water-Soluble Organic Li-Ion Battery Electrodes. *Electrochem. Commun.* **2013**, *34*, 174−176.
(10) Fédèle, L.; Sauvage, F.; Bois, J.; Tarascon, J.-M.; Bécuwe, M. Lithium Insertion/De-Insertion Properties of π-Extended Naphthyl-Based Dicarboxylate Electrode Synthesized by Freeze-Drying. *J. Electrochem. Soc.* **2014**, *161*, A46−A52.
(11) Han, X.; Chang, C.; Yuan, L.; Sun, T.; Sun, J. Aromatic Carbonyl Derivative Polymers as High-Performance Li-Ion Storage Materials. *Adv. Mater.* **2007**, *19*, 1616−1621.
(12) Renault, S.; Geng, J.; Dolhem, F.; Poizot, P. Evaluation of Polyketones with N-cyclic Structure as Electrode Material for Electrochemical Energy Storage: Case of Pyromellitic Diimide Dilithium Salt. *Chem. Commun.* **2011**, *47*, 2414−2416.
(13) Sharma, P.; Damien, D.; Nagarajan, K.; Shaijumon, M. M.; Hariharan, M. Perylene-polyimide-based Organic Electrode Materials for Rechargeable Lithium Batteries. *J. Phys. Chem. Lett.* **2013**, *4*, 3192−3197.
(14) Wu, H.; Wang, K.; Meng, Y.; Lua, K.; Wei, Z. An Organic Cathode Material Based on a Polyimide/CNT Nanocomposite for Lithium Ikon Batteries. *J. Mater. Chem. A* **2013**, *1*, 6366−6372.
(15) Liang, Y.; Tao, Z.; Chen, J. Organic Electrode Materials for Rechargeable Lithium Batteries. *Adv. Energy Mater.* **2012**, *2*, 742−769.
(16) Song, Z.; Zhou, H. Towards Sustainable and Versatile Energy Storage Devices: an Overview of Organic Electrode Materials. *Energy Environ. Sci.* **2013**, *6*, 2280−2301.
(17) Nakahara, K.; Iriyama, J.; Iwasa, S.; Suguro, M.; Satoh, M.; Cairns, E. J. Al-laminated Film Packaged Organic Radical Battery for High-power Applications. *J. Power Sources* **2007**, *163*, 1110−1113.
(18) Nishide, H.; Oyaizu, K. Toward Flexible Batteries. *Science* **2008**, *319*, 737−738.
(19) Janoschka, T.; Hager, M. D.; Schubert, U. S. Powering up the Future: Radical Polymers for Battery Applications. *Adv. Mater.* **2012**, *24*, 6397−6409.
(20) Sukegawa, T.; Kai, A.; Oyaizu, K.; Nishide, H. Synthesis of Pendant Nitronyl Nitroxide Radical-Containing Poly(norbornene)s as Ambipolar Electrode-Active Materials. *Macromolecules* **2013**, *46*, 1361−1367.
(21) Sano, N.; Tomita, W.; Hara, S.; Min, C.-M.; Lee, J.-S.; Oyaizu, K.; Nishide, H. Polyviologen Hydrogel with High-Rate Capability for Anodes Toward an Aqueous Electrolyte-type and Organic-based Rechargeable Device. *ACS Appl. Mater. Interfaces* **2013**, *5*, 1355−1361.
(22) Chen, H.; Armand, M.; Demailly, G.; Dolhem, F.; Poizot, P.; Tarascon, J.-M. From Biomass to a Renewable $Li_xC_6O_6$ Organic Electrode for Sustainable Li-Ion Batteries. *ChemSusChem* **2008**, *1*, 348−355.
(23) Chen, H.; Poizot, P.; Dolhem, F.; Basir, N. I.; Mentré, O.; Tarascon, J.-M. Electrochemical Reactivity of Lithium Chloranilate *vs* Li and Crystal Structures of the Hydrated Phases. *Electrochem. Solid-State Lett.* **2009**, *12*, A102−A106.
(24) Chen, H.; Armand, M.; Courty, M.; Jiang, M.; Grey, C. P.; Tarascon, J.-M.; Dolhem, F.; Poizot, P. Lithium Salt of Tetrahydroxybenzoquinone: Toward the Development of a Sustainable Li-Ion Battery. *J. Am. Chem. Soc.* **2009**, *131*, 8984−8988.
(25) Barrès, A.-L.; Geng, J.; Bonnard, G.; Renault, S.; Gottis, S.; Mentré, O.; Frayret, C.; Dolhem, F.; Poizot, P. High-Potential Reversible Li Deintercalation in a Substituted Tetrahydroxy-*p*-benzoquinone Dilithium Salt: An Experimental and Theoretical Study. *Chem. - Eur. J.* **2012**, *18*, 8800−8812.
(26) Bonnard, G.; Barrès, A.-L.; Danten, Y.; Allis, D. G.; Mentré, O.; Tomerini, D.; Gatti, G.; Izgorodina, E. I.; Poizot, P.; Frayret, C. Experimental and Theoretical Studies of Tetramethoxy-*p*-benzoquinone: Infrared Spectra, Structural and Lithium Insertion Properties. *RSC Adv.* **2013**, *3*, 19081−19095.
(27) Liang, Y.; Zhang, P.; Yang, S.; Tao, Z.; Chen, J. Fused Heteroaromatic Organic Compounds for High-Power Electrodes of Rechargeable Lithium Batteries. *Adv. Energy Mater.* **2013**, *3*, 600−605.
(28) Swallow, A. J. In *Function of Quinones in Energy Conserving Systems*; Trumpower, B. L., Ed.; Academic Press: New York, 1982; Chapter 2, p 68.
(29) Peover, M. E. A Polarographic Investigation into the Redox Behaviour of Quinones: The Roles of Electron Affinity and Solvent. *J. Chem. Soc.* **1962**, 4540−4549.
(30) Charrouf, Z.; Guillaume, D. Phenols and Polyphenols from Argania spinosa. *Am. J. Food Technol.* **2007**, *2*, 679−683.
(31) Del Signore, A.; Romeo, F.; Giaccio, M. Content of Phenolic Substances in Basidiomycetes. *Mycol. Res.* **1997**, *101*, 552−556.
(32) Briggs, D. E. G. Molecular Taphonomy of Animal and Plant Cuticles: Selective Preservation and Diagenesis. *Philos. Trans. R. Soc. London, Ser. B* **1999**, *354*, 7−17.
(33) Yam, K.; D'Angelo, I.; Kalscheuer, R.; Zhu, H.; Wang, J.-X.; Snieckus, V.; Ly, L. H.; Converse, P. J.; Jacobs, W. R., Jr.; Strynadka, N.; Eltis, L. D. Studies of a Ring-Cleaving Dioxygenase Illuminate the Role of Cholesterol Metabolism in the Pathogenesis *Mycobacterium tuberculosis*. *PLOS Pathog.* **2009**, *5*, 1−12.
(34) Li, W.; Xie, D.; Frost, J. W. Benzene-Free Synthesis of Catechol: Interfacing Microbial and Chemical Catalysis. *J. Am. Chem. Soc.* **2005**, *127*, 2874−2882.
(35) Bonneau-Gubelmann, I.; Michel, M.; Besson, B.; Ratton, S.; Desmurs, J.-R. In *Industrial Chemistry Library*; Jean-Roger, D., Serge, R., Eds.; Elsevier: Amsterdam, 1996; Vol. *8*, pp 116−128.
(36) Wang, S.; Wang, L.; Zhang, K.; Zhu, Z.; Tao, Z.; Chen, J. Organic $Li_4C_8H_2O_6$ Nanosheets for Lithium-Ion Batteries. *Nano Lett.* **2013**, *13*, 4404−4409.